

Experimental evidence of chemical components in the bonding of helium and neon with neutral molecules

David Cappelletti^{*1}, Alessio Bartocci¹, Felice Grandinetti², Stefano Falcinelli³, Leonardo Belpassi⁴, Francesco Tarantelli^{1,4} and Fernando Pirani¹

¹*Dipartimento di Chimica, Biologia e Biotecnologie, Università degli Studi di Perugia, via Elce di Sotto 8, 06123 Perugia, Italy*

²*Dipartimento per la Innovazione nei sistemi Biologici, Agroalimentari e Forestali (DIBAF), Università della Tuscia, 01100 Viterbo, Italy*

³*Dipartimento di Ingegneria Civile ed Ambientale, Università degli Studi di Perugia, 06125 Perugia, Italy*

⁴*Istituto di Tecnologia e Scienze Molecolari del CNR, via Elce di Sotto 8, 06123 Perugia Italy*

*(corresponding author) david.cappelletti@unipg.it;

Abstract: *The complexes of helium and neon with gaseous neutral molecules are generally perceived as van der Waals adducts, held together by physical (non covalent) forces, due to the combination of size (exchange) repulsion with dispersion/induction attraction. The molecular beam experiments discussed in the present article confirmed that this is the case for He-, Ne-CF₄ adducts, but revealed that the interaction of He and Ne with CCl₄ features an appreciable contribution of chemical components, arising from the anisotropy of the electron density of CCl₄ that enhances a charge transfer from Ng (Ng = He, Ne). These findings furnish a novel assay of the bonding capabilities of helium and neon, and invite to revisit the neutral complexes of these elements as systems of chemical relevance. The CCl₄-Ng are also peculiar examples of halogen bonds, a group of interactions of major current concern. Finally, our investigation preludes to the development of semi-empirical models for force fields aimed to the unified description of static and dynamical properties of systems of comparable or higher complexity.*

1. Introduction

Since Bartlett's synthesis¹ of $\text{Xe}^+\text{PtF}_6^-$, numerous compounds of the heavier noble gases have been isolated and structurally characterized.^{2,3,4,5} In 2000, Räsänen and coworkers⁶ detected HArF, a matrix compound with a covalent H-Ar bond. Helium and neon also form covalent ionic species,⁷ but, to date, no neutral compounds of these elements have been reported. Over the years, theory has unraveled several strategies to attempt the fixation of the lightest noble gases, particularly helium.⁸⁻¹¹ These proposals, however, must contend with the fragility of the predicted species, and the envisioning of suitable conditions for their preparation. In this regard, the recent detection in cold matrices of NeAuF^{12} and NeBeS^{13} is an important experimental progress. It is also well known¹⁴ that helium and neon form gaseous complexes with open- and closed-shell atoms, ions and simple molecules. These systems, however, are generally perceived as physically bound. They feature, indeed, very small binding energies, and are typically characterized as van der Waals (vdW) adducts. Chemical contributions were revealed in gas phase water-heavier noble gas systems, while no experimental evidence was found for complexes involving He and Ne.¹⁵ Interestingly, the high-resolution molecular beam (MB) scattering experiments discussed in this paper suggest that while $\text{CF}_4\text{-He}$, -Ne behave as typical vdW complexes, the interaction potentials of the apolar CCl_4 with He and Ne are properly described only when additional terms with respect to the vdW behavior are included. According to theoretical calculations, these phenomenological corrections actually reflect electronic effects, including the anisotropy of the charge distribution around the Cl atoms, and the occurrence of charge-transfer effects. Thus, despite their low intrinsic stability, $\text{CCl}_4\text{-He}$ and $\text{CCl}_4\text{-Ne}$ must be viewed as prototypical neutral adducts held together by weak chemical forces adding to vdW. This caught occurrence of chemical interaction components in neutral complexes of helium and neon puts these systems into a novel perspective, and

furnishes a novel assay of the bonding capabilities of these elements. Our results are also of interest in the context of the halogen-bond, a currently “hot” topic of major experimental and theoretical concern.¹⁶ Finally, the very small size of our sampled interactions could be a useful experimental benchmark to probe the performance of computational methods aimed at highly accurate analysis of chemical bonding.

2. Results and Discussion

The contribution of charge transfer (CT) marks the transition from physical to chemical intermolecular interactions. The CT effects are, however, often elusive to an accurate experimental/theoretical determination, as they can contribute to the bond stabilization in the perturbative limit. In any case, their evaluation becomes certainly more feasible, if they contribute significantly to the overall interaction. In this regard, the complexes of the apolar CF_4 and CCl_4 with a noble gas atom (Ng) are ideally suited model systems. In fact, due to their high symmetry (T_d), the interaction of CF_4 and CCl_4 with Ng features a reduced number of contributing components,¹⁵ making the ensuing complexes suitable to assess strength and anisotropic character of the ubiquitous vdW contribution (V_{vdW}). In addition, in the absence of electrostatic effects, and due to the minor role at large and intermediate intermolecular distances of induction terms, the in case contribution of CT becomes in principle a relevant part of the probed interaction. As a matter of fact, the major goal of the present work was the experimental assay of these CT contributions, successfully caught for the CCl_4 -He and CCl_4 -Ne complexes. The measured quantity is the total (elastic plus inelastic) integral cross section $Q(v)$ as a function of the MB velocity v for He and Ne colliding with CF_4 and CCl_4 (details in SI). The use of high velocity and high angular resolution conditions allows to catch the “glory” quantum interference, observed in the velocity dependence of the integral cross section. The experimental data provide information on the potential energy surface (PES) in

terms of absolute scale of the total intermolecular interaction, and on its radial and the angular dependences.

The $Q(v)$ data of the $\text{CCl}_4\text{-Ng}$ and $\text{CF}_4\text{-Ng}$ ($\text{Ng}=\text{He}$ and Ne , Fig.1) are clearly different, both in magnitude and in the interference pattern, highlighting pronounced differences in the intermolecular interactions.¹⁷ The dashed and the full lines are calculated $Q(v)$ assuming, respectively, a vdW interaction (non-covalent nature), and adding contributions of covalent nature (essentially CT) to the intermolecular interaction.

The intermolecular interaction, V , has been modeled considering four interaction centers located at the four C-Cl and C-F bonds, respectively, which generate four additive Ng-bond interaction terms (see SI). The vdW interaction energy here includes a repulsion term due to an *effective* molecular size,^{18,19} strongly dependent on the molecular orientation, and an attractive term determined by the combination of Ng-bond dispersion contributions.^{19,20} This approach exploits both the whole molecular polarizability and its partition in bond tensor components,²¹ and provides a realistic picture of both the repulsive and the attractive components of V_{vdW} . It includes also both effective three body and other non additive effects,^{19,20} and its performance was extensively assayed by comparison with *ab initio* results²²⁻²⁶.

The parameters of each Ng-bond pair (Tables S1 and S2) have been predicted by exploiting the bond polarizability, whose tensor components²¹ ($\alpha_{\parallel} = 3.67 \text{ \AA}^3$, $\alpha_{\perp} = 2.08 \text{ \AA}^3$ for C-Cl, and $\alpha_{\parallel} = 1.02 \text{ \AA}^3$, $\alpha_{\perp} = 0.57 \text{ \AA}^3$ for C-F) relate, respectively, to the size and shape of the electronic charge distribution around each bond.^{19,21} These have been combined with those of Ng ($\alpha_{\text{He}} = 0.2 \text{ \AA}^3$ and $\alpha_{\text{Ne}} = 0.4 \text{ \AA}^3$)²⁷ in correlation formulas^{18,19} so to estimate the V_{vdw} parameters. The latter were inserted into the ILJ formulation (see SI) with the additional constrain to asymptotically reproduce the *ab initio* dispersion coefficients.²⁸

The dynamical treatment adopted in the present work has been extensively exploited in the past to describe molecular collisions involving relatively large molecules in the thermal energy range.²⁹⁻³¹ Herein, the cross sections, measured in the 20-400 meV collision energy range, probe the interaction at intermediate and large intermolecular distances. The collision dynamics has been confined within two different regimes, defined by: *i*) a *spherical model*, where the molecule behaves as a “pseudo-atom”, and the scattering, mostly elastic, is driven by a central (radial) field, and *ii*) an *anisotropic molecular model*, where the cross section is represented as a combination of independent contributions from limiting configurations of the collision complex²⁹⁻³¹. In particular, vertex, edge, and face configurations, related to the basic cuts of the PES of a molecule of T_d symmetry, have been selected as representative of the interaction anisotropy. Accordingly, the two regimes selectively emerge as a function of the ratio between the mean rotation time, τ_M , and the collision time, τ_{coll} . In general, in a scattering experiment a short τ_M is required to probe an effective potential close to the isotropic component of the PES, which can be estimated as average of interactions associated to the limiting configurations of the collision complex ($\tau_M \approx 10^{-12}$ s and 10^{-13} s for CCl_4 and CF_4 , respectively, at $T = 300$ K). τ_{coll} has been found^{29,32} to range between 2×10^{-12} s and 5×10^{-13} s as the MB velocity v is varied from 0.5 km s^{-1} to 2.2 km s^{-1} .

The dynamical treatment based on the Ng-bond representation of V_{vdw} nicely reproduces the cross section measurements for $\text{CF}_4\text{-He}$ and $\text{CF}_4\text{-Ne}$ (dashed lines in Fig.1). This finding confirms the reliability of the employed methodology, and indicates the occurrence of a pure vdW interaction in these systems. By contrast, the same approach is unable to reproduce the experimental data of $\text{CCl}_4\text{-He}$ and $\text{CCl}_4\text{-Ne}$, measured with the same methodology under the same conditions. In particular, the glory structures calculated using simply V_{vdw} (dashed lines in Fig.1) are clearly shifted at velocities lower than the experimental values. It is well known¹⁷ that this happens when the binding energy of the collision complex, specifically the depth of

the interaction potential well, is underestimated. Any further attempt to fit the experimental data by simply varying the potential parameters, even well outside reasonable limits suggested by the correlation formulas,^{18,19} was unsuccessful. The best fit of the observed glory pattern was only achieved when two substantial modifications of the potential formulation were introduced. Interestingly, these two additional contributions have a clear chemical significance. The first takes into account the anisotropic character of the electron density in molecules containing heavier halogen atoms. It was in fact suggested³³ that along a carbon-halogen bond the halogen atom behaves as a “flattened sphere”, originating a “polar flattening” (PF) zone which is often associated with a positive electrostatic potential, the so-called “ σ -hole”. This zone is usually considered to affect the electrostatic interaction component that is however absent in the present systems. To account for PF contributions, we decreased the position of the repulsive wall of each Ng-bond pair in the parallel configuration by about 4%. The obtained effect was the increase of the potential well of the vertex geometries of CCl₄-He and CCl₄-Ne, those mainly probed by the present experiments. As a consequence, the anisotropic size repulsion decreases, accompanied by an increased weight of the dispersion attraction. The PF correction was, in particular, applied so to obtain a size change (Figs. S1 and S2) consistent with that extracted from the scattering experiments involving state-selected Cl atom MB and He or Ne targets.³⁴ Such experiments demonstrated that the Cl-He and Cl-Ne interactions are essentially of the vdW type. It was also possible to appraise the difference (anisotropy) in strength and range that originates from the different alignment (parallel or perpendicular) of the half-filled orbital of the Cl atom with respect to the intermolecular axis³⁴.

Despite the correction for the anisotropy of the electron density somewhat improved the fitting of the experimental data, it was insufficient to fully reproduce the measurements. Recently¹⁵ we showed that CT effects play a significant role in the stabilization of the bonding

in various types of gas-phase binary complexes involving hydrogenated molecules. Therefore, we included a further stabilizing contribution, arising in particular from stereo-selective CT effects (V_{CT}). This term, assumed to depend on the overlap integral between external orbitals of the interacting partners and then expected to be stereo-selective, has been formulated as an exponential which decreases with the distance r :

$$V_{CT} = -A \cos^4(\alpha) \exp(-\gamma r) \quad (1)$$

The value of γ , which defines^{35,36} at each molecular orientation the falloff of V_{CT} as He or Ne separate from the Cl atoms in CCl_4 , was assumed to coincide with that obtained for Cl-heavier Ng atom complexes, where strength, range and anisotropy of CT were so far explored in great detail.³⁴⁻³⁷ Therefore, the best fit of the experimental cross sections required to adjust only the pre-exponential factor A . Cross sections calculated with the modified V are plotted as full lines in Figure 1. The intermolecular potential so obtained for the basic configurations of CCl_4 -He, Ne systems are plotted in Fig.2, where results of the pure vdW component and of the complete interaction, including PF and CT, are compared. Note that the global reduction of the repulsive wall position affects mostly the vertex configuration (about 0.4-0.5 Å) and that the PF correction accounts for about one third of the full change (Fig. S2).

The results of the phenomenological analysis was also supported by high level quantum chemical calculations, performed to characterize selected cuts of the PES and to analyze the electronic density displacements that accompany the formation of the CCl_4 -Ng (Ng = He, Ne) in comparison with that occurring in the formation of homologous systems with CF_4 . Guided by the experiments, we focused our analysis on the three basic configurations, representative of the anisotropic behavior of PES for these systems (vertex, edge and face configuration).

In order to achieve interaction energies in the right scale of the experimental determination has been mandatory the use of extremely large basis sets in combination with quantum-

mechanical methods that include the electron correlation at the highest level of theory. Our first principle calculations reproduce properly the relative position of the minima for all systems in their basic configurations. The geometrical features are not significantly sensitive to the size of the basis set employed, whereas more challenging is to achieve properly converged values for the interaction energies. The computed values systematically decrease with the increasing basis set size employed (Tables S3, S4, S5) and the reference data (CCSD(T)/CBS) still lightly overestimate (deviations are of the order of 1-2 meV, i. e. 0.1-0.2 kJ/mol) the values obtained from the analysis of the experimental data, which indeed emerge as a very stringent test case to probe the performance in terms of accuracy of highly correlated quantum-mechanical methods based on first principles.

Now we move to the theoretical study of electron density changes taking place upon the formation of the adducts, $\text{CCl}_4\text{-Ng}$, aimed to analyze the occurrence of CT. In general, to put assay the presence of CT in weakly-interacting systems, it is necessary to assess and reliably compute effects arising from quite small changes in the electron density distribution. To tackle this problem, we recently proposed an approach, which offers a broad perspective in which to assess the presence of CT, free of any charge decomposition scheme. This is based on the key idea of a charge-displacement (CD) function,^{5,15} defined as

$$\Delta q(z) = \int_{-\infty}^{\infty} dx \int_{-\infty}^{\infty} dy \int_{-\infty}^z \Delta \rho(x, y, z') dz'$$

where $\Delta \rho$ is the difference between the electron density of the complex and that of the isolated non-interacting constituting fragments (specifically, Ng and CCl_4) placed in the same positions they occupy in the complex. Clearly, Δq measures, at each point z along a chosen axis, the electron charge that, upon formation of the complex, is displaced from right to left across the plane perpendicular to z and its values are fast converging with the size of the basis set employed.^{5,15} This provides a concise and insightful snapshot of the whole electron cloud

rearrangement arising from all the interaction components, and allows to unambiguously appraise the whole spatial extent and the chemical relevance of charge fluctuation and of transfer phenomena. In particular for weakly bound systems, the evaluation of $\Delta q(z)$ along an axis joining the interacting species is immediately helpful for a quantitative assessment of the occurrence and extent of CT, because the curve obviously suggests CT when it is appreciably different from zero and does not change sign in the region between fragments.

Fig.3 reports the CD curves obtained for $\text{CCl}_4\text{-He}$ and $\text{CCl}_4\text{-Ne}$ in the vertex, edge and face configurations. The intermolecular distance has been fixed to the value mainly probed by the experiments that is 4.8 Å for both He and Ne adducts.

The results clearly indicate the occurrence of an appreciable CT from Ng towards the CCl_4 (Δq is positive, corresponding to a flux of electron charge from right to left) just in the vertex configuration, for which as discussed before the experiments revealed indeed a sensitive additional intermolecular bond stabilization. The effect is clearly evident for He, and becomes even more pronounced for Ne. In the other hand, in the case of the edge and face arrangement, the CD curves are very close to zero both at the CCl_4 site and in the whole inter-fragment region where indeed cross the zero axis. Note that the same feature was found for prototypical van der Waals complexes as Xe-Ar (see Ref. 15). The patterns of CD curves clearly point out that the CT contributions in these configurations are negligible (at least at the distances mainly probed by the experiments) and strongly support the experimental findings described above where indeed the energy stabilization due to CT in the edge and face arrangements of $\text{CCl}_4\text{-He}$, -Ne (Fig.3) and in all the configurations of $\text{CF}_4\text{-He}$, -Ne (Fig. S3) is negligible.

Finally, we show that the analysis of the electron density gives surprisingly simple and sound justification of the shift in the position of the repulsion wall at the C-Cl site used in the analysis of the experimental data. Fig.4 (upper panel) compares the electron density at the Cl

site of CCl_4 with that of the *spherical* Cl atom (at the same position, origin of the axis) for selected isodensities. Interestingly, the formation of the C-Cl bond produces, at the chlorine atom site, a substantial decrease of electron density along the extension the C-Cl bond axis at the opposite side of the carbon. This electron depletion favors a closer approach of the electron-donor Ng atom along the CCl_4 vertex, leading to stronger attraction. If we choose a reference isodensity contour for CCl_4 , it crosses the axis (z) at values smaller than that for isolated Cl atom. We may expect that the difference in the crossing position, Δz (Å), may give an estimation of the shift in the position of the repulsion wall related to the PF. The Δz values, reported as a function of the reference isodensity contour value, are given in the lower panel of Figure 4. These estimated values are fully consistent with the shift of the repulsive wall introduced phenomenologically in the formulation of our potential (Fig. S2).

3. Conclusions

In conclusion, our high-resolution MB scattering experiments unraveled a case study of transition in the bonding nature for neutral complexes of helium and neon. Interestingly, and somewhat in contrast with simple chemical intuition, such transition neither results in large interaction energies (the strength of the full interaction falls in the scale of few meV), nor implies peculiar features of the binding partner. Rather, the small anisotropy of the electron density of the apolar CCl_4 is sufficient to enhance a charge transfer from Ng, and to shift from the *vdW* CF_4 -Ng to the *partial chemical* CCl_4 -Ng. Put in the perspective, these findings invite to revisit the “physical” neutral complexes of helium and neon as systems of conceivable chemical interest. Taking into account the variety of already observed species,³⁸⁻⁴⁰ the emerging bonding motifs could be numerous and different. The detailed investigation of these motifs could help to develop semi-empirical models aimed to the unified description of static

and dynamical properties of systems of comparable⁴¹ or higher complexity and to improve the mapping of transition from vdW to chemical bond.^{35,36}

Finally, being the intermolecular halogen bonding a fast-growing research field, connecting a wide range of subjects, from materials science to structural biology,⁴²⁻⁴⁴ the experimental characterization of anisotropy effects at halogen site may be of general relevance. Specifically, the determination of the shift of the V_{vdw} repulsive wall, the consequent dispersion attraction increase and CT effects, here characterized in prototypical halogenated systems, shall permit a more rational design and a proper formulation of new force fields.⁴⁵

4. Experimental section

The MB experimental apparatus has been extensively described previously.^{30,31} Shortly, it is composed by a set of differentially pumped vacuum chambers where the MB (He or Ne in the present experiments) is produced by a gaseous expansion from a nozzle. The source pressure is typically less than 10 mbar, and its temperature is varied in a wide range (90-500 K). In the expansion region, the MB is collimated by two skimmers and by a circular slit defining its angular divergence. Further downstream is analyzed in velocity by a mechanical selector formed by six slotted disks. The velocity-selected projectile atoms collide with a stationary target gas (in the present case, CCl_4 or CF_4) contained in the scattering chamber ($\approx 10^{-3}$ - 10^{-4} mbar), and are detected by a quadrupole mass spectrometer coupled with an ion counting setup. In these experiments the scattering chamber is kept at room temperature to avoid condensation effects on its walls and to maintain the rotational temperature sufficiently high to reduce inelastic events and to better resolve the glory amplitudes.

The fundamental quantity measured at each selected nominal velocity v is the MB attenuation I/I_0 , where I and I_0 represent, respectively, the MB intensity detected with and without the

target in the scattering chamber. The integral cross section $Q(\nu)$ is obtained from I/I_0 through the Lambert-Beer law.

In the data analysis procedure, center-of-mass cross sections have been calculated within the semi-classical JWKB method⁴⁶ from the assumed intermolecular interaction, and then convoluted in the laboratory frame to make a direct comparison with the measured $Q(\nu)$.

5. Computational methods

The interaction energies and the geometrical structures were obtained using the coupled cluster method with single, double, and perturbative triple excitations (CCSD(T)), in combination with the complete basis set (CBS) limit extrapolation (from augmented correlation-consistent polarized valence basis sets, aug-cc-pVTZ, aug-cc-pVQZ, and aug-cc-pV5Z).^{47,48} All computational details and the numerical results are reported in SI (see Table S3).

Acknowledgements

This work was supported by the Italian Ministero dell'Istruzione, della Ricerca e dell'Università (PRIN 2010-2011, grant 2010ERFKXL_002).

- ¹ N. Bartlett, *Proc. Chem. Soc.* **1962**, 218.
- ² J. F. Lehmann, H. P. A. Mercier, G. J. Schrobilgen, G. J. *Coord. Chem. Rev.* **2002**, 233-234, 1-39.
- ³ W. Grochala, *Chem. Soc. Rev.* **2007**, 36, 1632-1655.
- ⁴ A. S. Cooke, M. C. Gerry, *J. Am. Chem. Soc.* **2004**, 126, 17000-17008.
- ⁵ L. Belpassi, I. Infante, F. Tarantelli, L. Visscher, *J. Am. Chem. Soc.* **2008**, 130, 1048-1060.
- ⁶ L. Khriachtchev, M. Pettersson, N. Runeberg, J. Lundell, M. Räsänen, *Nature* **2000**, 406, 874-876.
- ⁷ F. Grandinetti, *Int. J. Mass Spectrom.* **2004**, 237, 243-267.
- ⁸ W. Koch, G. Frenking, J. Gauss, D. Cremer, J. R. Collins, *J. Am. Chem. Soc.* **1987**, 109, 5917-5934.
- ⁹ M. H. Wong, *J. Am. Chem. Soc.* **2000**, 122, 6289-6290.
- ¹⁰ H. S. Rzepa, *Nature Chemistry* **2010**, 2, 390-393.
- ¹¹ W. Grochala, *Phys. Chem. Chem. Phys.* **2012**, 14, 14860-14868.
- ¹² X. Wang, L. Andrews, F. Brogi, S. Riedel, *Chem.-Eur. J.* **2013**, 19, 1397-1409.
- ¹³ Q. Wang, X. Wang, *J. Phys. Chem. A* **2013**, 117, 1508-1513.
- ¹⁴ F. Pirani, G. S. Maciel, D. Cappelletti, V. Aquilanti, *Int. Rev. Phys. Chem.* **2006**, 19, 165-199.
- ¹⁵ D. Cappelletti, E. Ronca, L. Belpassi, F. Tarantelli, F. Pirani, *Acc. Chem. Res.* **2012**, 45, 1571-1580.
- ¹⁶ A. Legon, *Phys. Chem. Chem. Phys.* **2010**, 12, 7736.
- ¹⁷ F. Pirani, S. Brizi, L. F. Roncaratti, P. Casavecchia, D. Cappelletti, F. Vecchiocattivi, *Phys. Chem. Chem. Phys.* **2008**, 10, 5489-5503.
- ¹⁸ R. Cambi, D. Cappelletti, G. Liuti, F. Pirani, *J. Chem. Phys.* **1991**, 95, 1852-1861.

- ¹⁹ F. Pirani, D. Cappelletti, G. Liuti, G. Range, *Chem. Phys. Lett.* **2001**, *350*, 286 – 296.
- ²⁰ F. Pirani, M. Albertí, A. Castro, M. M. Teixidor, D. Cappelletti, *Chem. Phys. Lett.* **2004**, *394*, 37–44.
- ²¹ K. Denbigh, *Trans. Farad. Soc.* **1940**, *36*, 936–948.
- ²² M. Albertí, A. Aguilar, J. M. Lucas, F. Pirani, D. Cappelletti, C. Coletti, N. Re, *J. Phys. Chem. A* **2006**, *110*, 9002–9010.
- ²³ M. Albertí, A. Aguilar, J. M. Lucas, F. Pirani, C. Coletti, N. Re, *J. Phys. Chem. A* **113**, 14606–14614 (2009).
- ²⁴ L. F. Roncaratti, L. Belpassi, D. Cappelletti, F. Pirani, F. Tarantelli, *J. Phys. Chem. A* **2009**, *113*, 15223–15232.
- ²⁵ M. Alberti, A. Amat, F. De Angelis, F. Pirani, *J. Phys. Chem. B* **2013**, *117*, 7065-7076.
- ²⁶ M. Bartolomei, E. Carmona-Novillo, M. I. Hernández, J. Campos-Martínez, F. Pirani, *J. Phys. Chem. C* **2013**, *117*, 10512–10522.
- ²⁷ T. N. Olney, N. Cann, G. Cooper, C. Brion, *Chem. Phys.* **1997**, *223*, 59 – 98.
- ²⁸ A. Kumar, *J. Mol. Struct. (Theochem)* **2002**, *591*, 91 – 99.
- ²⁹ D. Cappelletti, M. Bartolomei, F. Pirani, V. Aquilanti, *J. Phys. Chem. A* **2002**, *106*, 10764-10772.
- ³⁰ F. Pirani, M. Bartolomei, V. Aquilanti, M. Scotoni, M. Vescovi, D. Ascenzi, D. Bassi, D. Cappelletti, *J. Chem. Phys.* **2003**, *119*, 265–276.
- ³¹ D. Cappelletti, M. Bartolomei, M. Sabido, F. Pirani, G. Blanquet, J. Walrand, J.-P. Bouanich, F. Thibault, *J. Phys. Chem. A* **2005**, *109*, 8471–8480.
- ³² V. Aquilanti, D. Ascenzi, D. Cappelletti, M. de Castro, F. Pirani, *J. Chem. Phys.* **1998**, *109*, 3898–3910.
- ³³ P. Politzer, P. Lane, M. C. Concha, Y. Ma, J. S. Murray, *J. Mol. Model.* **2007**, *13*, 305–311.

- ³⁴ V. Aquilanti, D. Cappelletti, V. Lorent, E. Luzzatti, F. Pirani, *J. Phys. Chem.* **1993**, *97*, 2063–2071.
- ³⁵ F. Pirani, A. Giulivi, D. Cappelletti, V. Aquilanti, *Mol. Phys.* **2000**, *98*, 1749–1762.
- ³⁶ V. Aquilanti, D. Cappelletti, F. Pirani, *Chem. Phys. Lett.* **1997**, *271*, 216–222.
- ³⁷ V. Aquilanti, D. Cappelletti, F. Pirani, *J. Chem. Soc., Faraday Trans.* **1993**, *89*, 1467–1474.
- ³⁸ M. Chałasiński, M. M. Szczyński, *Chem. Rev.* **1994**, *94*, 1723-1765, and other references in this issue.
- ³⁹ R. M. Balabin, *Chem. Phys.* **2008**, *352*, 267-275.
- ⁴⁰ S. Pakhira, D. Mandal, B. Mondal, A. K. Das, *Struct. Chem.* **2012**, *23*, 681-692.
- ⁴¹ A. Rohrbacher, K. C. Janda, L. Beneventi, P. Casavecchia, *J. Chem. Phys.* **1997**, *101*, 6528-6537.
- ⁴² P. Metrangolo, G. Resnati, *Science* **2008**, *121*, 918-919.
- ⁴³ M. Erdelyi, *Nature Chemistry* **2014**, *6*, 762-764.
- ⁴⁴ A. R. Voth, P. Khuu, K. Oishi, P. Shing Ho, *Nature Chem.* **2009**, *1*, 74-79.
- ⁴⁵ M. Carter, K. Rappé, P. Shing Ho, *J. Chem. Theory Comput.* **2012**, *8*, 2461-2473.
- ⁴⁶ M.S. Child, *Molecular collision theory*. Academic Press London and New York, **1974**.
- ⁴⁷ T. H. Dunning, *J. Chem. Phys.* **1989**, *90*, 1007–1023.
- ⁴⁸ D.E. Woon, T.H. Dunning, *J. Chem. Phys.*, **1993**, *98*, 1358–1371.

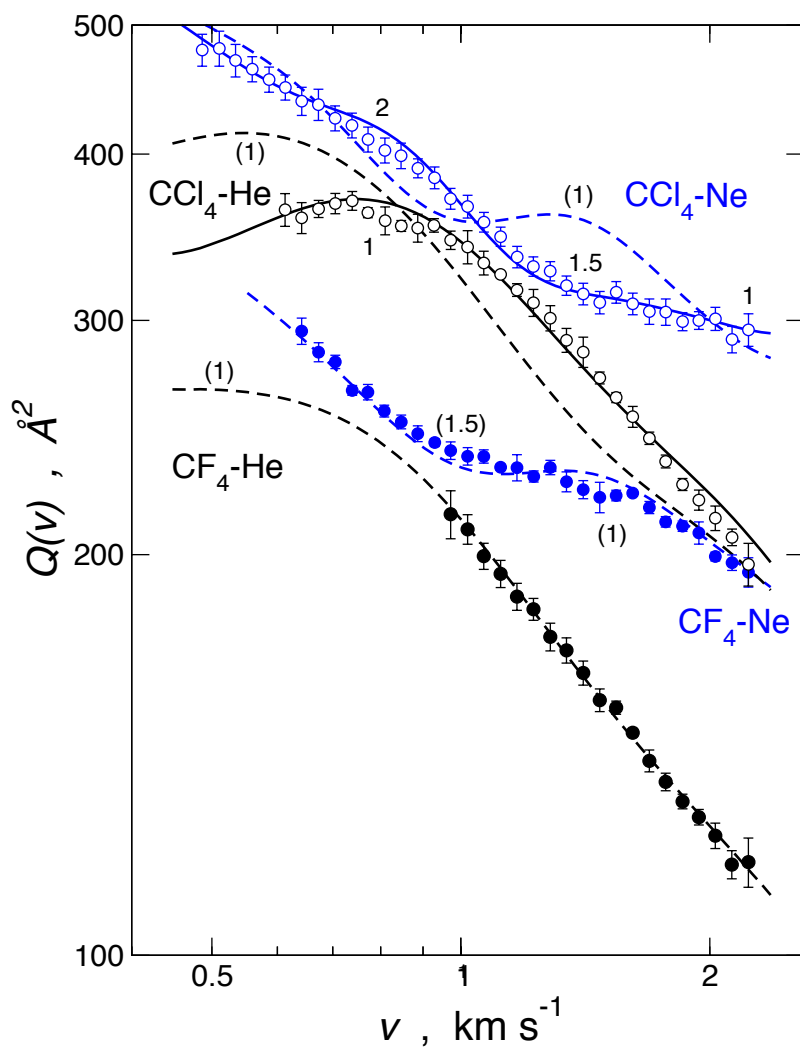


Figure 1 - **Integral cross sections** - for the $\text{CCl}_4\text{-Ng}$ and $\text{CF}_4\text{-Ng}$ ($\text{Ng} = \text{He}, \text{Ne}$) measured as a function of the MB velocity v ($1 \text{ \AA} = 0.1 \text{ nm}$). Vertical error bars represent \pm two standard deviations. Full and dashed lines represent, respectively, the results of the data analysis performed including and excluding chemical contributions to the intermolecular interaction (see text). The numbers indicate the glory extreme orders¹⁷ and those in parenthesis refer to calculations using only the V_{vdw} interaction component.

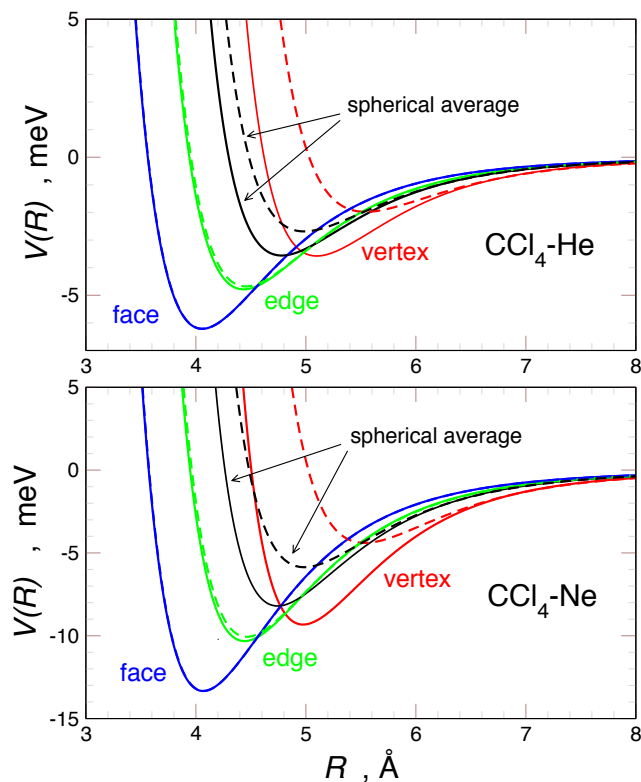


Figure 2 - **Intermolecular potentials** - for the $\text{CCl}_4\text{-Ng}$ ($\text{Ng} = \text{He}, \text{Ne}$) plotted as a function of R , the distance between the center of mass of two partners. Three basic configurations of the PES, the vertex (red), the edge (green), and the face (blue) are represented together with the spherical average of the full PES (black). The dashed and the full lines are, respectively, pure vdW interactions (non-covalent), and the full interaction including the two additional chemical contributions (PF and CT, see text). PF amounts to about one third of the overall interaction ($1 \text{ meV} = 0.096485 \text{ kJ/mol}$).

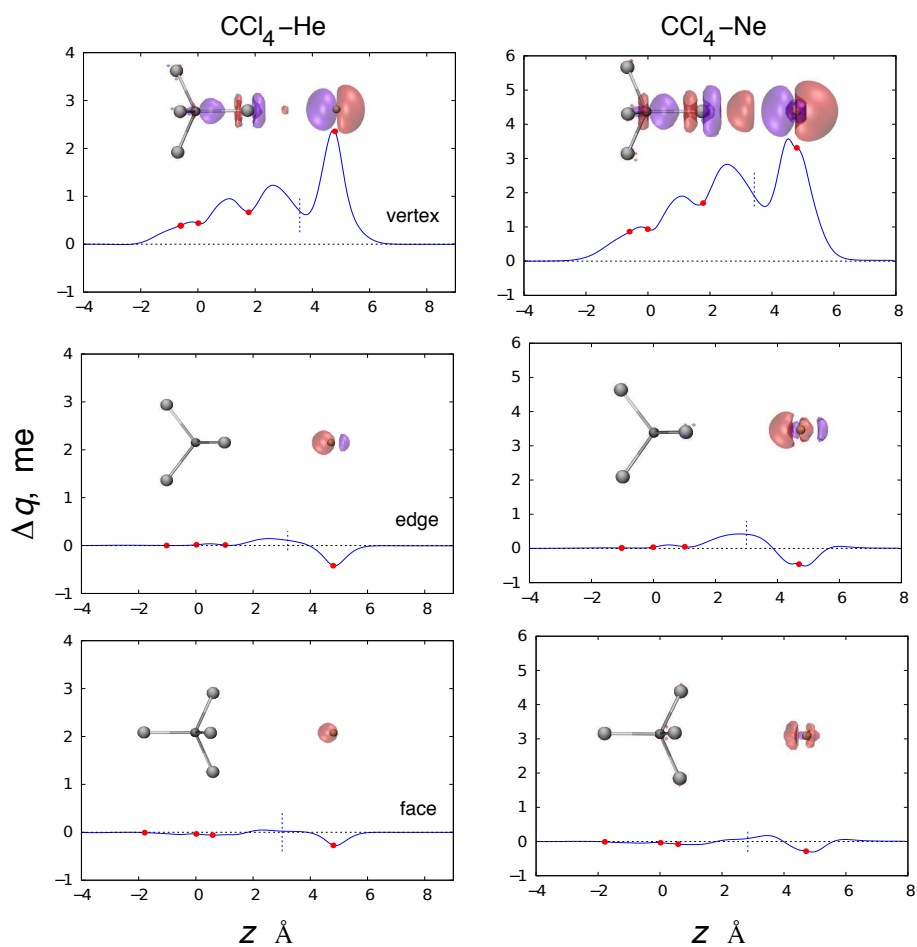


Figure 3 - **Charge displacement curves** - for three basic configurations of the $\text{CCl}_4\text{-Ng}$ ($\text{Ng} = \text{He}, \text{Ne}$). 3D contour plots of the electron density change accompanying bond formation are also shown, with isodensity surfaces for $\Delta\rho \pm 5 \times 10^{-5} \text{ e/bohr}^3$ (negative value in red, positive value in blue). The dots on the Δq curves mark the projection of the nuclear positions on the z axis, which is here the axis joining Ng with the c.m. of CCl_4 . The axis origin is at the C atom of CCl_4 , and He or Ne are placed at the experimental averaged distance (4.8 \AA from C). Vertical dashed lines mark the isodensity boundaries between the fragments where CT has been evaluated.

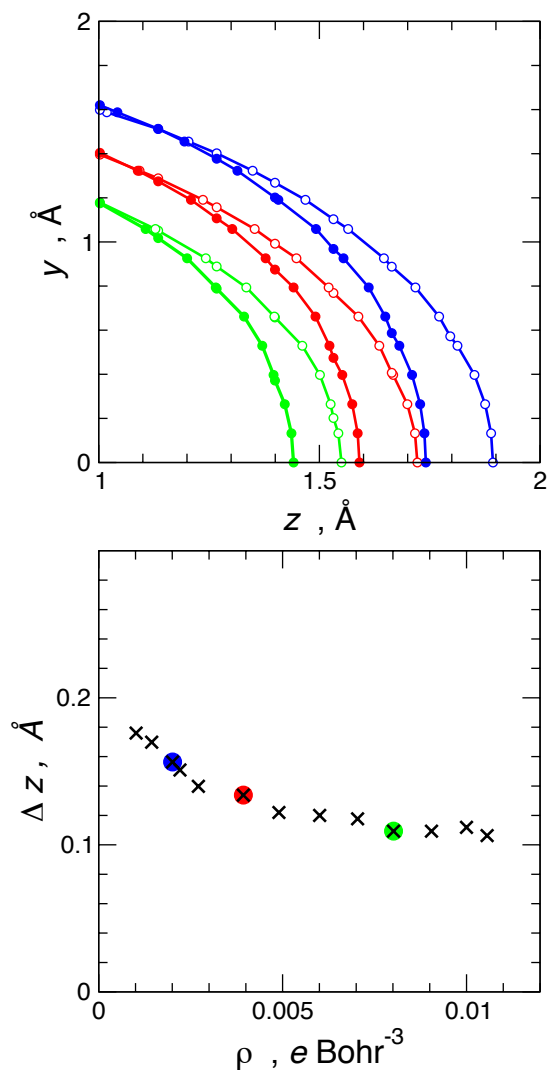


Figure 4 - **Electronic densities** - The upper panel compares the 2D contour plots of the electronic density of CCl_4 (full circles) and of the isolated (spherical) Cl atom (open circles), placed at the same position of the bonded Cl, for three representative isodensity surfaces. The lower panel shows the Δz (Å) (see text for details) behavior for the Cl- CCl_4 (crosses) as a function of the isodensity value (e/bohr^3). The colored circles correspond to the isodensity contours shown in the upper panel. The same analysis performed on F- CF_4 provides Δz close to zero.